Appl. Phys. B 75, 621–627 (2002)
DOI: 10.1007/s00340-002-1007-4

Applied Physics B
Lasers and Optics

Spectral broadening of 40-fs Ti:sapphire laser pulses in photonic-molecule modes of a cobweb-microstructure fiber

A.B. FEDOTOV[1]
P. ZHOU[2]
A.N. NAUMOV[1]
V.V. TEMNOV[2]
V.I. BELOGLAZOV[3]
N.B. SKIBINA[3]
L.A. MEL'NIKOV[3]
A.V. SHCHERBAKOV[3]
A.P. TARASEVITCH[2]
D. VON DER LINDE[2]
A.M. ZHELTIKOV[1,✉]

[1] Physics Department, International Laser Center, M.V. Lomonosov Moscow State University, 119 899 Moscow, Russia
[2] Institut für Laser- und Plasmaphysik, Universität Essen, 45 117 Essen, Germany
[3] Institute of Glass Structure Technology and Equipment, pr. Stroitelei 1, 410 044 Saratov, Russia

Received: 9 June 2002/Revised version: 29 June 2002
Published online: 22 November 2002 •

ABSTRACT Photonic-molecule modes of a cobweb-microstructure fiber allow efficient nonlinear optical spectral broadening of nanojoule femtosecond light pulses. Spectral widths of approximately 200 nm are achieved at the output of a 6-cm sample of such a fiber for 40-fs Ti:sapphire laser pulses with an energy of a few nanojoules coupled into photonic-molecule modes. Higher values of the group index and a lower group-velocity dispersion, attainable with higher-order photonic-molecule modes, allow the efficiency of spectral broadening of femtosecond laser pulses to be increased relative to the efficiency of spectral broadening in the fundamental photonic-molecule mode.

PACS 42.65.Wi; 42.81.Qb

1 Introduction

The capability of microstructure (MS) fibers [1–12] to enhance the whole catalogue of basic nonlinear optical phenomena has recently resulted in several important breakthroughs in modern science, in fact opening a new chapter in optical physics and making nonlinear optics accessible to unamplified femtosecond pulses. Although the first MS fibers were created in the early 1970s [13, 14], it was not until recently that the potential of such fibers for nonlinear and ultrafast optics, as well as optical metrology and biomedical applications, has been fully realized. Due to the high degree of light confinement in the fiber core attainable with MS fibers [15–17], nonlinear optical effects can now be observed with sub-nanojoule femtosecond pulses and fiber samples with a length of several centimeters [16–20]. Supercontinuum generation using low-energy light pulses [6, 21, 22] is one of the most impressive achievements of nonlinear optics of microstructure fibers, which has important implications in optical metrology [23–26] and optical coherence tomography [27–29] and which is being studied very intensely in the context of pulse compression [30], numerous spectroscopic applications [10], and the analysis of fundamental aspects of nonlinear fiber optics and soliton physics [31]. Microstructure fibers have also been shown to result in the enhancement of self- and cross-phase modulation [15, 16, 19, 32], as well as third-harmonic generation [18, 19, 32]. The possibilities of using microstructure fibers and polycapillary arrays for high-order harmonic generation [4, 33] as well as for guiding, focusing, and compressing ultra-short X-ray pulses [34] are now being explored. Due to the progress in fiber technologies, this direction of nonlinear optics is developing in parallel with high-field nonlinear optics, allowing very efficient spectral transformations of light pulses, opening the ways to control the phase and the spectrum of short pulses [35], and competing with high-field physics in the generation of ultra-short pulses and synthesis of few-cycle field waveforms.

The core–cladding configuration determines many of the functional abilities of microstructure fibers. In particular, although the effects related to strong light confinement show up in microstructure fibers with different geometries, the degree of light localization in the fiber core and, hence, the degree to which nonlinear optical processes are enhanced depend on the air-filling fraction of the cladding [16, 17], which determines the effective refractive index of the cladding. Microstructure fibers with a photonic-crystal cladding provide new regimes of waveguiding due to a high reflectivity of the cladding around the photonic band gap [4, 36] and allow many of the ideas discussed in connection with photonic crystals (see e.g. [37–40]) to be realized. The possibility to design microstructure fibers with different configurations of the core and the cladding helps to engineer and tailor the dispersion of such fibers [2, 6, 10, 20, 41–45], which is of special value for nonlinear optics and short-pulse formation and control. A hole-assisted microstructured fiber, comprising a material index profile for waveguiding and air holes for modifying optical properties, has been demonstrated recently [46] to allow an anomalous dispersion larger than that of conventional fibers to be achieved without introducing large optical losses. With a special design of the core and the cladding, a microstructure fiber can be made highly birefringent [47], as was demonstrated, for example, for a cobweb photonic-crystal (PC) fiber [48]. This opens the ways, as shown recently by Apolonski et al. [49], for polarization control of supercontinuum generation.

In this paper, we will present the results of nonlinear optical experiments performed with MS fibers whose core has the form of a cyclic photonic molecule (PM) in its cross section

✉ Fax: +7-095/939-3959, E-mail: zheltikov@top.phys.msu.su

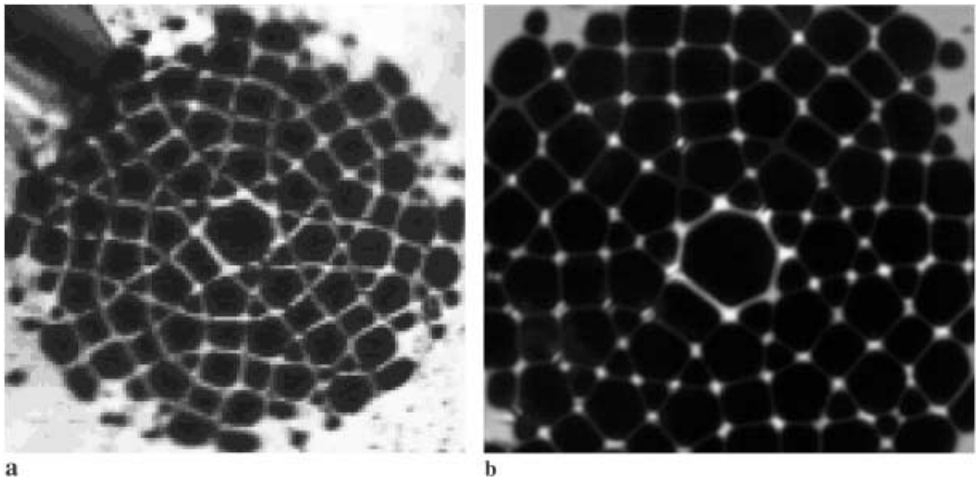

FIGURE 1 **a** A cross-sectional image of a photonic-molecule microstructure-integrated bundle of fibers with a radius of each fiber in the bundle equal to 2 μm and the distance between the neighboring fibers of 7.4 μm. **b** The spatial distribution of light intensity in the fundamental photonic-molecule mode excited with helium–neon laser radiation in a cobweb-microstructure fiber shown in **a**

(Fig. 1a). Air holes arranged in a two-dimensionally periodic structure in the cladding of this fiber and a larger hole at the center of the fiber form a cyclic-molecule-like structure, consisting of an array of small-diameter glass channels linked by narrow bridges, around the central hole (Fig. 1a). This photonic-molecule microstructure-integrated bundle of fibers can guide the light through total internal reflection (Fig. 1b), providing a very high light-confinement degree due to the large refractive-index step. We will show that fibers of this type offer new solutions to the key problem of nonlinear waveguide optics of very short light pulses, opening new ways to engineer waveguide dispersion. We will demonstrate below that the photonic-molecule analogy provides very useful insights into the properties of dispersion and waveguide modes in MS fibers with a special design of the fiber core, permitting a better understanding of dispersion-tailoring and field-distribution aspects and allowing the potentialities of such fibers in the context of nonlinear optical applications to be assessed.

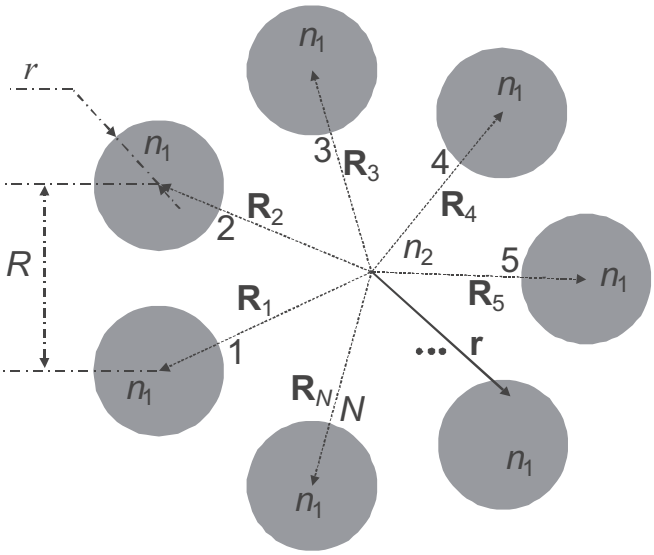

FIGURE 2 A photonic-molecule model for an optical fiber where the light is guided along a set of N cores with the refractive index n_1 surrounded by a material with the refractive index n_2 and linked by narrow bridges with the distance between the neighboring cores equal to R

2 Photonic-molecule modes of a cobweb-microstructure fiber

In this section, we will discuss the properties of waveguide modes of a cobweb MS fiber (Fig. 1a) with a thin ring-like wall separating the central hole from the rest of the structure and with a very high refractive-index step between this ring and the adjacent areas, which is achieved due to the high air-filling fraction of the microstructure. In contrast to earlier work (e.g. [4, 50]), we are interested in the light guided along this narrow ring surrounding the hollow core of this fiber. Thus, instead of air-guided modes, considered in a very illuminating way by Cregan et al. [4], we consider the modes of the cladding of a hollow-core MS fiber. This cladding, as is readily seen from Fig. 1a,b, can be considered as an array of standard circular bare fiber cores linked by narrow bridges. Such a configuration of fiber cores linked by bridges is reminiscent of the configuration of atoms linked by chemical bonds in a cyclic polyatomic molecule consisting of identical atoms (a generic diagram of such a two-dimensional molecule is shown in Fig. 2), which brings us to an idea of using a photonic-molecule analogy to understand the optical properties of such a waveguiding structure (this approach was outlined earlier [45, 51]). The physics behind the analogy between a bundle of coupled MS-integrated fibers and a polyatomic molecule is that the way the distribution of the refractive index in the plane of Fig. 2, showing the cross section of a bundle of coupled fibers, modulates the light field is similar to the way the distribution of potential in a polyatomic molecule modifies the electron wave function. Mathematically, this analogy stems from the similarity of coupled-theory equations for an array of fibers [52] and perturbation-theory equations for the electron wave function in a polyatomic molecule. Earlier, an elegant model of a diatomic photonic molecule has been used to describe the modes of coupled semiconductor [53] and dye-doped polymer [54] microcavities. Below, we will extend this analogy by introducing a two-dimensional polyatomic photonic molecule. This effort will later prove to be quite rewarding by providing us with an illustrative and physically clear model of dispersion properties and mode structure of the considered rather complicated optical fiber.

The main purpose of the analysis performed in this section is to use the photonic-molecule analogy to qualitatively explain the general features of dispersion and mode structure of an optical fiber where the light is guided along a set of N channels with the refractive index n_1 (Fig. 2) surrounded by a material with the refractive index n_2 and linked by narrow bridges. The fiber channels, forming a two-dimensional photonic molecule in the plane of Fig. 2, are made of glass whose wavelength dependence of the group index is given by curve 1 in Fig. 3. We start our analysis with a set of N isolated single-mode fibers consisting of a bare core surrounded with air. As long as these fibers remain isolated, the dispersion relation of such an array is degenerate (curve 2 in Fig. 3), and this degeneracy is N-fold. As soon as we allow them to be coupled to each other, the degeneracy is partially or completely lifted, similar to polyatomic molecules consisting of identical atoms, giving rise to several dispersion branches (curves 3–6 in Fig. 3).

We will restrict ourselves to a scalar-wave-equation approximation in this paper, ignoring at this stage many of potentially useful polarization effects. The modes of the PM fiber can then be represented as superpositions of modes of isolated fibers forming our structure:

$$\Psi(\boldsymbol{r}) = \sum_n A_n f\,(\boldsymbol{r} - \boldsymbol{R}_n), \tag{1}$$

where $\boldsymbol{r}$ is the radius vector in the plane of the fiber cross section (the plane of Fig. 2), $\boldsymbol{R}_n$ are the coordinates of the nth fiber center (Fig. 2), and A_n and f are the amplitude and the transverse distribution of the field for the nth fiber.

Since only the neighboring fibers are coupled to each other in our two-dimensional photonic molecule (Fig. 1a,b), the coupled-mode equations for the field amplitudes [52, 55] can be written as

$$\frac{\mathrm{d}A_n}{\mathrm{d}z} - \mathrm{i}\beta A_n - \mathrm{i}\alpha\left(A_{L(n)} + A_{R(n)}\right) = 0, \tag{2}$$

where β is the propagation constant for the relevant mode of an isolated fiber,

$$\alpha = \frac{\omega^2}{2\beta c^2}\frac{\int \Delta\varepsilon(\boldsymbol{r}) f\,(\boldsymbol{r} - \boldsymbol{R}_{n'})\, f^*\,(\boldsymbol{r} - \boldsymbol{R}_n)\,\mathrm{d}\boldsymbol{r}}{\int |f\,(\boldsymbol{r} - \boldsymbol{R}_n)|^2\,\mathrm{d}\boldsymbol{r}} \tag{3}$$

(ω is the radiation frequency and $\Delta\varepsilon(\boldsymbol{r})$ is the deviation from the unperturbed dielectric constant $\varepsilon_2 = n_2^2$ at a given point with a radius vector $\boldsymbol{r}$) is the coefficient characterizing mode coupling in nth and n'th fibers, and

$$L(n) = \begin{cases} n-1, & n > 0 \\ N, & n = 0 \end{cases},$$

$$R(n) = \begin{cases} n+1, & n < N \\ 1, & n = N \end{cases}.$$

The propagation constants can now be found from the characteristic equation corresponding to the set of (2). In the general case of arbitrary N, these propagation constants can be calculated with the use of numerical methods. There are several simple analytical solutions, however, that provide useful physical insights into the dispersion of the PM fiber. In particular, a symmetric field distribution,

$$\Psi_1(\boldsymbol{r}) = A\sum_n f\,(\boldsymbol{r} - \boldsymbol{R}_n)\,, \tag{4}$$

where A is a constant, is allowed by (2) for any N. This symmetric mode of our fiber is similar to a symmetric wave function of a polyatomic molecule. The propagation constant for such a symmetric mode is given by the formula

$$B_1 = \beta + 2\alpha, \tag{5}$$

which shows that mode coupling in the considered array of fibers results in a renormalization of propagation constants, leading to the increase in the propagation constants in the case of the totally symmetric mode of a PM fiber (curve 3 in Fig. 3).

An antisymmetric solution

$$\Psi_N(\boldsymbol{r}) = A\sum_n (-1)^n\, f\,(\boldsymbol{r} - \boldsymbol{R}_n) \tag{6}$$

is also allowed by (2) for even N. This antisymmetric mode also has an obvious analogy in quantum chemistry. The propagation constant is then renormalized in accordance with

$$B_N = \beta - 2\alpha. \tag{7}$$

By analogy with the classification of modes in a standard fiber (see e.g. [55]), we identify the fundamental mode of our photonic-molecule fiber as the mode with the largest propagation constant. The highest value of the propagation constant in the case of our PM fiber is achieved for the symmetric mode (curve 3 in Fig. 3). This mode will, therefore, be referred to as the fundamental mode. We introduce the mode index l to enumerate PM-fiber modes, which will be denoted as PM$_l$ modes, starting with $l = 1$, which corresponds to the fundamental PM mode.

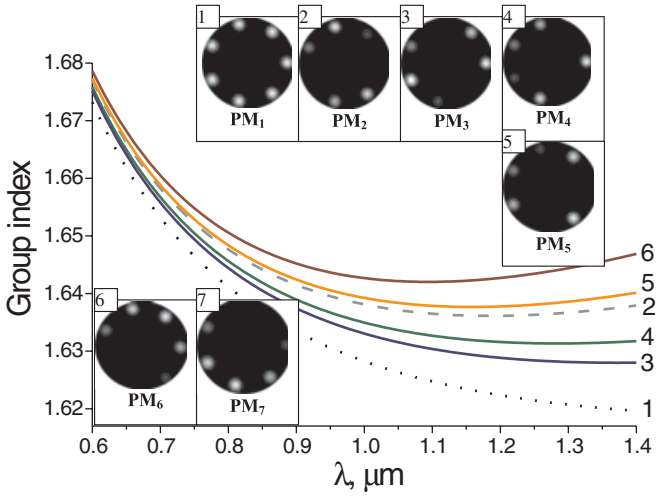

FIGURE 3 The group index as a function of radiation wavelength for (1) the material of the fiber; (2) a single isolated fiber from the considered photonic-molecule structure (or an array of identical fibers completely isolated from one another); and (3) PM_1, (4) PM_2 and PM_3, (5) PM_4 and PM_5, and (6) PM_6 and PM_7 modes of a seven-core photonic-molecule fiber ($N = 7$). The radius of a single fiber in the photonic-molecule cobweb structure is 2 μm and the distance between the neighboring fibers in the photonic-molecule structure is 7.4 μm. The *insets* show light-intensity distributions in (1) PM_1, (2) PM_2, (3) PM_3, (4) PM_4, (5) PM_5, (6) PM_6, and (7) PM_7 modes of a seven-core photonic-molecule structure

3 Dispersion properties of photonic-molecule modes

Our model of the fiber structure employed in our experiments (Fig. 1a) consisted of seven identical glass cores with a radius of 2 μm. The refractive index of the cladding was set equal to the refractive index of atmospheric-pressure air, since the air-filling fraction of the structure was very high (see Fig. 1a). The distance R between the neighboring cores was estimated as 7.4 μm. To estimate the coupling coefficient appearing in (2), we employed the expression for the coupling coefficient, $\alpha = C\lambda$ (where λ is the wavelength), from the model of two coupled identical planar waveguides [55]. For characteristic geometric sizes of our structure, this model allows the parameter C to be estimated as $0.016\,\mu\text{m}^{-2}$. Only lowest-order modes of isolated fibers were included in our calculations. The inclusion of higher-order modes will, of course, change dispersion branches of a PM fiber and make the analysis much more complicated. The model that includes only fundamental modes of each elementary fiber, on the other hand, allows the general physical features of dispersion of a PM fiber to be understood without reproducing the fiber dispersion in all the details.

Photonic-molecule modes of our MS fiber differ from each other by their dispersion properties, which implies that the efficiency of nonlinear optical processes in these modes should also be different. Figure 3 presents the group indices of PM_l fiber modes calculated with the use of the above-described model. The field-intensity distributions corresponding to these modes are shown in insets 1–7 in Fig. 3. Generally, the waveguide dispersion, as can be seen from Fig. 3, may be changed quite substantially by exciting different PM_l modes of a photonic-molecule fiber. In particular, the zero group-velocity point can be shifted to approximately 950 nm for the slowest, PM_6 and PM_7, modes of a seven-atom photonic-molecule fiber (curve 6 in Fig. 3). These higher-order modes are, therefore, much better suited for nonlinear experiments involving the propagation of femtosecond Ti:sapphire laser pulses than the fundamental PM mode. As can be seen from the results of numerical simulations presented in Fig. 3, higher-order PM fiber modes are also characterized by higher values of the group index, which implies that nonlinear optical processes should be enhanced for such slow modes. In particular, the efficiency of nonlinear optical interactions for the PM_6/PM_7 degenerate fiber mode shown in insets 6 and 7 in Fig. 3 should be noticeably higher than the efficiency of nonlinear optical processes for the fundamental, symmetric PM_1 mode, shown in inset 1 in Fig. 3.

Thus, we should point out here two factors leading to the enhancement of nonlinear optical processes in higher-order PM_l modes relative to lower-order PM modes: (i) the larger shift of the zero group-velocity dispersion wavelength, characteristic of higher-order PM modes and (ii) the higher group indices and, consequently, lower group velocities attainable with higher-order PM modes. The importance of shifting the zero group velocity dispersion wavelength and achieving the regime of anomalous dispersion for efficient spectral broadening and supercontinuum generation has been demonstrated by earlier experiments with both holey [6] and tapered [56, 57] fibers. The lowest values of the group index, as can be seen from the results of numerical simulations presented in Fig. 3, are achieved for PM_l-fiber modes with smooth profiles. The propagation constant and the group velocity of PM-fiber modes decrease with the growth in the number of extrema in the spatial profile of the PM-fiber mode. Obviously, the number of fibers in a PM-fiber bundle define the upper bound for the number of such extrema in the profile of the PM_l-fiber mode. The decrease in the group velocity for uneven PM_l-fiber modes implies that nonlinear optical processes should be enhanced for such slow modes. This expectation has been fully justified by the results of our experiments on supercontinuum generation in PM fibers, presented in Sect. 5. Thus, although the analysis performed in this section is valid, rigorously speaking, only for a bundle of single-mode fibers, it provides very useful physical insights into the possibilities of controlling nonlinear optical processes in PM fibers through the excitation of different modes of such fiber structures.

4 Experimental

Spectral broadening of short pulses propagating in photonic-molecule modes of MS fibers was studied in our experiments with the use of femtosecond pulses produced by a Ti:sapphire laser system. This laser system included a Ti:sapphire master oscillator and a regenerative amplifier and was capable of generating 40-fs pulses of 800-nm radiation with an energy up to 0.2 mJ per pulse and a repetition rate of 1 kHz. Special measures were taken to precompensate for pulse distortions in order to exclude the contribution of initial pulse-shape distortions to the asymmetry of self-phase modulation-induced spectral broadening of light pulses in an MS fiber.

The details of the technology employed to fabricate MS fibers used in our experiments, which was similar to the process developed by Knight et al. [1], were described elsewhere [58]. Briefly, the fabrication process involved drawing identical glass capillaries stacked into a periodic preform at an elevated temperature, cutting the resulting structure into segments, and repeating the technological cycle again. This procedure allowed the fabrication of microstructure fibers with different configurations of the core and the cladding and different spatial scales of the structure. In particular, cobweb fibers with the design shown in Fig. 1b have been fabricated with the diameter of the photonic-molecule ring at the center of the fiber ranging from 4 up to 20 μm.

The energy of light pulses coupled into photonic-crystal fibers was varied with the use of calibrated neutral-density filters. The laser beam was focused on the entrance face of a fiber sample, placed on a three-dimensional translation stage, with a micro-objective. Radiation emerging from the fiber was collimated with an identical micro-objective and was split into two beams. One of these beams was delivered to a spectrograph, while the other was used to visualize the waveguide mode excited in a PM fiber by imaging the light-field distribution at the output end of the fiber onto a CCD camera. This allowed us to examine the influence of the mode structure on the efficiency of spectral broadening of Ti:sapphire pulses in the fiber.

The procedure of PM fiber mode excitation included the angular alignment of the light beam and the fiber sample, the adjustment of the fiber input end position in three coordinates,

and the optimization of the beam-focus position by shifting the focusing micro-objective along the light-beam axis. The fundamental PM mode was excited in our experiments by focusing the laser beam to the center of the PM ring of the fiber. Laser radiation was then trapped by the thin glass wall of this central ring and was uniformly distributed over the glass channels forming a two-dimensional photonic molecule. Higher-order modes were excited by shifting the front end of the fiber with respect to the focused laser beam. The efficiency of radiation coupling into PM fiber modes achieved with such a procedure was typically on the order of several per cent. The improvement in the efficiency of PM fiber mode excitation requires a more precise matching of the light-field distribution in the input plane of the fiber and the geometry of the waveguiding structure, which could be apparently achieved by means of diffractive optics.

5 Results and discussion

Varying the focusing geometry and shifting the fiber end with respect to the light beam coupled into the fiber, we were able to excite, in fact, all the PM_l fiber modes with $l = 1, 2, \ldots, 7$. We observed efficient self-phase modulation and spectral broadening for all these modes excited by 40-fs pulses of 780-nm Ti:sapphire laser radiation in 6-cm PM-fiber samples. The increase in the energy of laser pulses coupled into the fiber allowed broader spectra of output radiation to be achieved with the same fiber sample and the same initial conditions at the input end of the fiber (Fig. 4). With 40-nJ Ti:sapphire laser pulses coupled into the MS fiber, the spectra of pulses emerging from the fiber had the full width approaching 200 nm.

Spectrally broadened radiation emerging from the fiber was imaged onto a CCD camera, placed behind a set of neutral-density filters. The insets in Fig. 5 provide examples of the light-field distribution at the output fiber end corresponding to the PM_1 (right) and PM_6/PM_7 (left) modes, excited by varying the initial conditions at the input end of the fiber. Higher-order PM modes, characterized by lower group velocities and a weaker group-velocity dispersion (see Fig. 3), enabled us to achieve larger values of spectral broadening for the same energies of laser pulses coupled into the fiber (cf. curves 2 and 3 in Fig. 5). The spectra of output radiation were noticeably narrower when Ti:sapphire laser pulses with the same energy were coupled into the fundamental PM_1 mode of the MS fiber (curve 2 in Fig. 5).

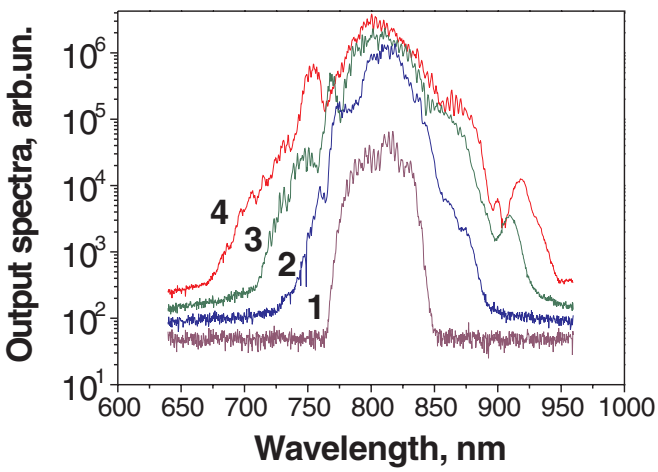

FIGURE 4 The spectra of (1) the input Ti:sapphire laser pulse and (2)–(4) radiation emerging from the PM_6/PM_7 modes of the cobweb fiber with a length of 4.5 cm. The energy of the laser pulse coupled into the fiber is (2) 12, (3) 21, and (4) 32 nJ. The radius of a single fiber in the photonic-molecule cobweb structure is 2 μm and the distance between the neighboring fibers in the photonic-molecule structure is 7.4 μm

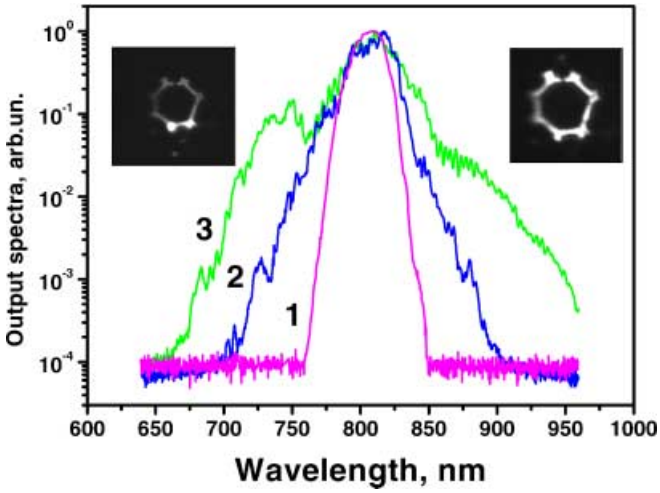

FIGURE 5 The spectra of (1) the input Ti:sapphire laser pulse and (2), (3) radiation emerging from (2) the PM_1 and (3) the PM_6/PM_7 modes of the cobweb-microstructure fiber with a length of 4.5 cm. The initial duration of the light pulses is 40 fs, and the energy coupled into the PM modes is estimated as 30 nJ. The radius of a single fiber in the photonic-molecule cobweb structure is 2 μm and the distance between the neighboring fibers in the photonic-molecule structure is 7.4 μm. The *insets* show the images of the light-intensity distribution at the output of the fiber corresponding to the PM_1 (*right*) and PM_6/PM_7 (*left*) modes

To estimate the time duration of laser pulses emerging from the microstructure fiber and to get a qualitative understanding of the influence of group-delay effects on the process of spectral broadening, we measured the cross-correlation function by mixing spectrally broadened radiation pulses emerging from the fiber with the fundamental radiation pulse of the Ti:sapphire laser (the autocorrelation trace for this pulse is shown in the inset in Fig. 6) in a 100-μm BBO crystal. The curves 1 and 2 in Fig. 6 display the cross-correlation traces measured with the use of this technique for femtosecond pulses spectrally broadened in PM_1 and PM_6/PM_7 modes of the microstructure fiber. The results of these cross-correlation measurements demonstrate, as can be seen from the comparison of curves 1 and 2 in Fig. 6, that the light pulses emerging from higher-order PM modes are characterized by broader cross-correlation traces and are delayed in time with respect to laser pulses spectrally broadened in the fundamental PM_1 mode. A detailed numerical model of spectral broadening is, of course, necessary to extract qualitative information from the comparison of these cross-correlation traces and the dispersion curves for PM modes presented in Fig. 3. Additional information on the chirp of spectrally broadened pulses emerging from the fiber would be necessary to accurately decode the results of cross-correlation measurements. However, some useful qualitative judgements can be made based on the comparison of the experimental cross-correlation traces and

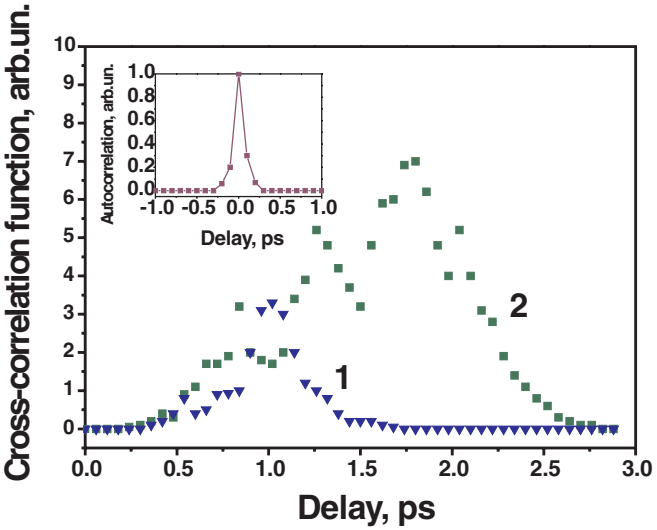

FIGURE 6 Cross-correlation traces measured by mixing radiation pulses spectrally broadened in (1) PM_1 and (2) PM_6/PM_7 modes of the microstructure fiber with the fundamental radiation pulse of the Ti:sapphire laser in a 100-μm BBO crystal. The *inset* shows an autocorrelation trace of the input Ti:sapphire laser pulse

our theoretical predictions concerning the group-index behavior in different PM modes. In particular, the cross-correlation traces presented in Fig. 6 show that the light pulse corresponding to the PM_6/PM_7 modes of the microstructure fiber is delayed in time with respect to the pulse with the PM_1-mode transverse intensity distribution. This is consistent with our model, which predicts lower group velocities for higher-order PM modes (see Fig. 3). The estimate of the delay time between the pulses emerging from the PM_6/PM_7 and PM_1 modes of the MS fiber obtained from the experimental cross-correlation traces is 0.7–0.9 ps. This agrees reasonably well with the results of group-index calculations for the studied PM modes presented in Fig. 3. To demonstrate this, we use a simple formula $\tau_g = (L\Delta n_g)/c$ to estimate the group-delay time τ_g between the PM_6/PM_7 and PM_1 mode pulses with the group-index difference Δn_g in an MS fiber with the length L (c is the speed of light). Then, inserting the values of $L = 4.5$ cm and $\Delta n_g = 6 \times 10^{-3}$ (cf. curves 3 and 6 in Fig. 3) into this formula, we arrive at an estimate of $\tau_g \approx 0.9$ ps for the group-delay time. The broader cross-correlation trace for higher-order PM modes, on the other hand, cannot be explained from the analysis of the group-velocity dispersion at the fundamental wavelength, as the group-velocity dispersion for higher-order PM modes is lower than that for the fundamental, PM_1 mode, and the zero-dispersion point in the case of higher-order modes lies closer to the fundamental wavelength. It should be taken into consideration, however, that the pulses propagating in higher-order PM modes are characterized by noticeably larger values of self-phase modulation-induced spectral broadening as compared to the pulses propagating in the fundamental, PM_1 mode (see Fig. 5). This leads to larger differences in group indices of different frequency components within self-phase modulation-broadened spectra and, hence, larger scatters in group delays, in the case of higher-order modes. This purely qualitative argument is, of course, not sufficient for the quantitative interpretation of the results of cross-correlation measurements, which could be provided on the basis of comparing the results of numerical simulations for the temporal evolution of laser pulses in PM modes with cross-correlation measurements performed on MS fibers of different lengths. Such an analysis falls beyond the scope of this paper.

Since the efficiency of radiation coupling into PM-fiber modes was typically at the level of several per cent in our experiments, optical breakdown on the input end of the fiber was the main limiting factor in our studies, which prevented us from approaching the regime of supercontinuum generation. We anticipate, therefore, that much larger spectral widths can be achieved at the output of PM fibers by improving the efficiency of radiation coupling into PM-fiber modes.

Because of a relatively large total effective area of PM modes in MS fibers, the efficiency of spectral broadening of femtosecond laser pulses in such modes is typically lower than the efficiency of spectral broadening in single-core holey and photonic-crystal fibers [6, 21, 22], as well as in tapered fibers [56, 57]. However, photonic-molecule modes of microstructure fibers studied in this paper offer several important options, which seem to advantageously supplement vast opportunities provided by photonic-crystal fibers. In particular, additional dispersion tunability can be achieved in the case of PM-fiber modes by varying the initial conditions at the input end of the fiber, resulting in the excitation of different PM-fiber modes. A promising direction for further studies would be to explore the possibility of coherent control of nonlinear optical cross-action processes in the fibers of a PM waveguiding structure by using pulses with different temporal and spatial profiles, frequencies, and initial chirps. It would be of interest also to search for new ways to phase match nonlinear optical interactions in such fibers, as well as to examine the potential of PM fibers for pulse compression through self- and cross-phase modulation and supercontinuum generation. The geometry of PM fibers is also advantageous for broadband evanescent-field spectroscopy and sensing of gases or liquids using supercontinuum generation, as well as for the laser guiding of atoms.

6 Conclusion

The analysis of optical properties of photonic-molecule modes in a microstructure fiber performed in this paper shows that the created cobweb-microstructure fibers are not only interesting objects for studying fundamental aspects of photon-localization modes in micro- and nanostructured matter and developing heuristic analogies with quantum chemistry, but also offer several new ways of dispersion engineering and switching between the regimes of nonlinear optical interactions. The dispersion branches, as shown above, are highly sensitive to the coupling constants characterizing the bonds in the photonic molecule. This allows the waveguide dispersion to be controlled by changing parameters of the bridges linking elementary glass channels in our structure. This possibility of dispersion engineering seems to offer much promise for nonlinear optical applications, allowing phase matching to be improved for various nonlinear optical processes. This fiber design is also very attractive for multiwave mixing, since pump waves may enter different cores of the central ring-like structure to interact then through the

bridges linking these cores. With the holes of our fiber structure filled with nonlinear or laser-active media, the evanescent field of guided modes can be used to generate nonlinear optical signals and produce the lasing effect. While all these ideas and possibilities still have to be analyzed in greater detail, the results of experiments presented in this paper provide an example of how nonlinear optical processes can be enhanced and controlled in photonic-molecule microstructure fibers, opening new avenues for applications of fiber-optic components in nonlinear optics and spectroscopy, optical metrology, and biomedicine, as well as offering new opportunities in generating ultra-short light pulses and few-cycle light-field waveforms and in controlling parameters of such pulses and waveforms.

ACKNOWLEDGEMENTS This study was supported in part by the President of the Russian Federation (Grant No. 00-15-99304), the Russian Foundation for Basic Research (Project No. 00-02-17567), and the Volkswagen Foundation (Project No. I/76 869). This material is based upon work supported by the European Research Office of the US Army under Contract No. N62558-02-M-6023.

REFERENCES

1 J.C. Knight, T.A. Birks, P.S.J. Russell, D.M. Atkin: Opt. Lett. **21**, 1547 (1996)
2 T.A. Birks, J.C. Knight, P.S.J. Russell: Opt. Lett. **22**, 961 (1997)
3 J.C. Knight, J. Broeng, T.A. Birks, P.S.J. Russell: Science **282**, 1476 (1998)
4 R.F. Cregan, B.J. Mangan, J.C. Knight, T.A. Birks, P.S.J. Russell, P.J. Roberts, D.C. Allan: Science **285**, 1537 (1999)
5 P.J. Bennet, T.M. Monro, D.J. Richardson: Opt. Lett. **24**, 1203 (1999)
6 J.K. Ranka, R.S. Windeler, A.J. Stentz: Opt. Lett. **25**, 25 (2000)
7 T.M. Monro, P.J. Bennett, N.G.R. Broderick, D.J. Richardson: Opt. Lett. **25**, 206 (2000)
8 A.B. Fedotov, A.M. Zheltikov, L.A. Mel'nikov, A.P. Tarasevitch, D. von der Linde: JETP Lett. **71**, 281 (2000)
9 M.V. Alfimov, A.M. Zheltikov, A.A. Ivanov, V.I. Beloglazov, B.A. Kirillov, S.A. Magnitskii, A.V. Tarasishin, A.B. Fedotov, L.A. Mel'nikov, N.B. Skibina: JETP Lett. **71**, 489 (2000)
10 A.M. Zheltikov: Phys. Usp. **170**, 1203 (2000)
11 M.A. van Eijkelenborg, M.C.J. Large, A. Argyros, J. Zagari, S. Manos, N.A. Issa, I. Bassett, S. Fleming, R.C. McPhedran, C. Martijn de Sterke, N.A.P. Nicorovici: Opt. Express **9**, 319 (2001)
12 K. Suzuki, H. Kubota, S. Kawanishi, M. Tanaka, M. Fujita: Opt. Express **9**, 676 (2001)
13 P. Kaiser, E.A.J. Marcatili, S.E. Miller: Bell Syst. Tech. J. **52**, 265 (1973)
14 P.V. Kaiser, H.W. Astle: Bell Syst. Tech. J. **53**, 1021 (1974)
15 N.G.R. Broderick, T.M. Monro, P.J. Bennett, D.J. Richardson: Opt. Lett. **24**, 1395 (1999)
16 A.B. Fedotov, A.M. Zheltikov, A.P. Tarasevitch, D. von der Linde: Appl. Phys. B **73**, 181 (2001)
17 A.M. Zheltikov, M.V. Alfimov, A.B. Fedotov, A.A. Ivanov, M.S. Syrchin, A.P. Tarasevitch, D. von der Linde: JETP **93**, 499 (2001)
18 J.K. Ranka, R.S. Windeler, A.J. Stentz: Opt. Lett. **25**, 796 (2000)
19 A.B. Fedotov, V.V. Yakovlev, A.M. Zheltikov: Laser Phys. **12**, 268 (2002)
20 B.J. Eggleton, C. Kerbage, P.S. Westbrook, R.S. Windeler, A. Hale: Opt. Express **9**, 698 (2001)
21 S. Coen, A.H.L. Chau, R. Leonhardt, J.D. Harvey, J.C. Knight, W.J. Wadsworth, P.S.J. Russell: Opt. Lett. **26**, 1356 (2001)
22 R. Holzwarth, M. Zimmermann, T. Udem, T.W. Hansch, P. Russbuldt, K. Gabel, R. Poprawe, J.C. Knight, W.J. Wadsworth, P.St.J. Russell: Opt. Lett. **17**, 1376 (2001)
23 S.A. Diddams, D.J. Jones, Jun Ye, S.T. Cundiff, J.L. Hall, J.K. Ranka, R.S. Windeler, R. Holzwarth, T. Udem, T.W. Hänsch: Phys. Rev. Lett. **84**, 5102 (2000)
24 D.J. Jones, S.A. Diddams, J.K. Ranka, A. Stentz, R.S. Windeler, J.L. Hall, S.T. Cundi: Science **288**, 635 (2000)
25 R. Holzwarth, T. Udem, T.W. Hänsch, J.C. Knight, W.J. Wadsworth, P.S.J. Russell: Phys. Rev. Lett. **85**, 2264 (2000)
26 S.N. Bagayev, A.K. Dmitriyev, S.V. Chepurov, A.S. Dychkov, V.M. Klementyev, D.B. Kolker, S.A. Kuznetsov, Y.A. Matyugin, M.V. Okhapkin, V.S. Pivtsov, M.N. Skvortsov, V.F. Zakharyash, T.A. Birks, W.J. Wadsworth, P.S.J. Russell, A.M. Zheltikov: Laser Phys. **11**, 1270 (2001)
27 A.A. Ivanov, M.V. Alfimov, A.M. Zheltikov: Laser Phys. **10**, 796 (2000)
28 A.A. Ivanov, M.V. Alfimov, A.B. Fedotov, A.A. Podshivalov, D. Chorvat, D. Chorvat, Jr., A.M. Zheltikov: Laser Phys. **11**, 158 (2001)
29 I. Hartl, X.D. Li, C. Chudoba, R.K. Rhanta, T.H. Ko, J.G. Fujimoto, J.K. Ranka, R.S. Windeler: Opt. Lett. **26**, 608 (2001)
30 A.V. Husakou, J. Herrmann: Phys. Rev. Lett. **87**, 203901-4 (2001)
31 J. Herrmann, U. Griebner, N. Zhavoronkov, A. Husakou, D. Nickel, J.C. Knight, W.J. Wadsworth, P.S.J. Russell, G. Korn: Phys. Rev. Lett. **88**, 173901-1 (2002)
32 A.N. Naumov, A.B. Fedotov, A.M. Zheltikov, V.V. Yakovlev, L.A. Mel'nikov, V.I. Beloglazov, N.B. Skibina, A.V. Shcherbakov: J. Opt. Soc. Am. B **19**, 2183 (2002)
33 A.N. Naumov, A.M. Zheltikov: IEEE J. Quantum Electron. **QE-32**, 129 (2002)
34 A.N. Naumov, A.M. Zheltikov: Laser Phys. **12**, 971 (2002)
35 A.N. Naumov, A.M. Zheltikov: Opt. Express **10**, 122 (2002)
36 J.C. Knight, T.A. Birks, R.F. Cregan, P.St.J. Russell, J.-P. De Sandro: Opt. Mater. **11**, 143 (1999)
37 E. Yablonovitch: J. Opt. Soc. Am. B **10**, 283 (1993)
38 J. Joannopoulos, R. Meade, J. Winn: *Photonic Crystals* (Princeton University Press 1995)
39 C.M. Soukoulis (Ed.): *Photonic Band Gaps and Localization* (Plenum, New York 1993)
40 M. Bertolotti, C.M. Bowden, C. Sibilia (Eds.): *Nanoscale Linear and Nonlinear Optics* (American Institute of Physics, New York 2001)
41 D. Mogilevtsev, T.A. Birks, P.St.J. Russell: Opt. Lett. **23**, 1662 (1998)
42 T.M. Monro, D.J. Richardson, N.G.R. Broderick, P.J. Bennett: J. Lightwave Technol. **17**, 1093 (1999)
43 A. Ferrando, E. Silvestre, J.J. Miret, J.A. Monsoriu, M.V. Andres, P.S.J. Russell: Electron. Lett. **24**, 325 (1999)
44 J.C. Knight, J. Arriaga, T.A. Birks, A. Ortigosa-Blanch, W.J. Wadsworth, P.S.J. Russell: IEEE Photon. Technol. Lett. **12**, 807 (2000)
45 A.B. Fedotov, A.N. Naumov, I. Bugar, D. Chorvat, Jr., D.A. Sidorov-Biryukov, D. Chorvat, A.M. Zheltikov: IEEE J. Sel. Top. Quantum Electron. **8**, 665 (2002)
46 T. Hasegawa, E. Sasaoka, M. Onishi, M. Nishimura, Y. Tsuji, M. Koshiba: Opt. Express **9**, 681 (2001)
47 A. Ortigosa-Blanch, J.C. Knight, W.J. Wadsworth, J. Arriaga, B.J. Mangan, T.A. Birks, P.S.J. Russell: Opt. Lett. **25**, 1325 (2000)
48 J.C. Knight, J. Arriaga, T.A. Birks, A. Ortigosa-Blanch, W.J. Wadsworth, P.S.J. Russell: IEEE Photon. Technol. Lett. **12**, 807 (2000)
49 A. Apolonski, B. Povazay, W. Drexler, W.J. Wadsworth, J.C. Knight, P.S.J. Russell: J. Opt. Soc. Am. B **19**, 2165 (2002)
50 J. Broeng, S.E. Barkou, T. Sondergaard, A. Bjarklev: Opt. Lett. **25**, 96 (2000)
51 A.B. Fedotov, A.N. Naumov, S.O. Konorov, V.I. Beloglazov, L.A. Mel'nikov, N.B. Skibina, D.A. Sidorov-Biryukov, A.V. Shcherbakov, A.M. Zheltikov: Laser Phys. **12**, 1191 (2002)
52 A. Yariv, P. Yeh: *Optical Waves in Crystals* (Wiley, New York 1987)
53 M. Bayer, T. Gutbrod, J.P. Reithmaier, A. Forchel, T.L. Reinecke, P.A. Knipp, A.A. Dremin, V.D. Kulakovskii: Phys. Rev. Lett. **81**, 2582 (1998)
54 T. Mukaiyama, K. Takeda, H. Miyazaki, Y. Jimba, M. Kuwata-Gonokami: Phys. Rev. Lett. **82**, 4623 (1999)
55 A.W. Snyder, J.D. Love: *Optical Waveguide Theory* (Chapman and Hall, New York 1983)
56 T.A. Birks, W.J. Wadsworth, P.S.J. Russell: Opt. Lett. **25**, 1415 (2000)
57 D.A. Akimov, A.A. Ivanov, M.V. Alfimov, S.N. Bagayev, T.A. Birks, W.J. Wadsworth, P.S.J. Russell, A.B. Fedotov, V.S. Pivtsov, A.A. Podshivalov, A.M. Zheltikov: Appl. Phys. B **74**, 307 (2002)
58 A.B. Fedotov, M.V. Alfimov, A.A. Ivanov, A.V. Tarasishin, V.I. Beloglazov, A.P. Tarasevitch, D. von der Linde, B.A. Kirillov, S.A. Magnitskii, D. Chorvat, D. Chorvat, Jr., A.N. Naumov, E.A. Vlasova, D.A. Sidorov-Biryukov, A.A. Podshivalov, O.A. Kolevatova, L.A. Mel'nikov, D.A. Akimov, V.A. Makarov, Y.S. Skibina, A.M. Zheltikov: Laser Phys. **11**, 138 (2001)